Investigation of Possible Structures of Silicon Nanotubes via Density-Functional Tight-Binding Molecular Dynamics Simulations and ab Initio Calculations

R. Q. Zhang

Center of Super-Diamond and Advanced Films (COSDAF) and Department of Physics and Materials Sciences, City University of Hong Kong, Hong Kong SAR, China

Ho-Lam Lee and Wai-Kee Li

Department of Chemistry, The Chinese University of Hong Kong, Shatin, New Territories, Hong Kong SAR, China

Boon K. Teo*

Department of Chemistry, University of Illinois at Chicago, 845 West Taylor Street, Chicago, Illinois 60607

We show, computationally, that single-walled silicon nanotubes (SiNTs) can adopt a number of distorted tubular structures, representing respective local energy minima, depending on the theory used and the initial models adopted. In particular, "gearlike" structures containing alternating sp^3-like and sp^2-like silicon local configurations have been found to be the dominant structural form for SiNTs via density-functional tight-binding molecular dynamics simulations (followed by geometrical optimization using Hartree−Fock or density function theory) at moderate temperatures (below 100 K). The gearlike structures of SiNTs deviate considerably from, and are energetically more stable than, the smooth-walled tubes (the silicon analogues of single-walled carbon nanotubes). They are, however, energetically less favorable than the "string-bean-like" SiNT structures previously derived from semiempirical molecular orbital calculations. The energetics and the structures of gearlike SiNTs are shown to depend primarily on the diameter of the tube, irrespective of the type (zigzag, armchair, or chiral). In contrast, the energy gap is very sensitive to both the diameter and the type of the nanotube.

1. Introduction

The past decade has seen intense efforts directed at studies of the structures and properties of tubular materials in the nanorealm. This interest is in part fueled by the discovery of carbon nanotubes (CNTs)[1,2] in the early 1990s. More recently, nanotubes of a wide variety of materials have been prepared. These one-dimensional materials often exhibit unusual physical and chemical properties with potential applications in catalysts, pharmaceuticals, and nanoelectronics, etc. Many noncarbon nanotubes have also been theoretically predicted or experimentally observed.[3−6] Unlike carbon nanotubes, the analogous silicon nanotubes, based on rolled-up graphene-like sheets, are yet to be made, though several theoretical investigations have appeared.[7−13]

The reason that low-dimensional silicon nanostructures have attracted much attention is due to their apparent compatibility with the silicon-based microelectronics and the prospects of becoming the most versatile building materials for nanoelectronic devices.[14−19] The natural question to ask is then why silicon and carbon, both belonging to the same group in the Periodic Table, behave so differently. It is well-known that silicon prefers diamond-like structures (with sp^3 hybridization) over graphite-like sheets (with sp^2 hybridization). In fact, one-dimensional silicon nanowires (SiNWs) have been routinely synthesized by various methods[20−23] and their interesting physical and chemical properties explored, whereas silicon nanotubes (SiNTs) based on rolled-up graphene-like sheets are yet to be made.

The possibility of the existence of SiNTs similar to the conventional CNTs had been studied theoretically by several groups.[7−13,19] On the basis of silicon's "inability" to adopt the sp^2 coordination, Seifert et al.[7] argued that the existence of SiNTs is doubtful. Alternatively, these authors proposed that Si-based silicide and SiH nanotubes are theoretically stable and energetically viable and could thus be considered as sources of silicon nanotubes, particularly in view of the existence of many layered silicides. On the other hand, by applying density functional theory (DFT), Fagan et al.[8] established theoretical similarities between silicon and carbon nanotubes. Their results showed that the electronic and structural properties of SiNTs are similar to those of CNTs; i.e., they may exhibit metallic or semiconductive behaviors, depending on the structure type (zigzag, armchair, or chiral) and the tube diameter. The strain energies of zigzag and armchair smooth SiNT structures have also been obtained by Barnard and Russo[9] on the basis of DFT calculations. In one of our recent publications,[19] we explored the possibility of the existence of SiNTs via semiempirical calculations. We found that SiNTs could in principle be formed with corrugated (along the tube axis) surfaces under appropriate conditions. In a more recent work, Zhang et al.[10] obtained similar corrugated tubular structures optimized by DFT calculations. It is obvious from these studies that the calculated structures of SiNTs are sensitive to the methods used.

The present work attempts to evaluate the structural and energetic characteristics of three different kinds (zigzag, armchair, and chiral) of single-walled SiNT structures by performing

density-functional tight-binding molecular dynamics (DFTB-MD) simulations at various select temperatures. Confirmation of some of the findings was done by ab initio Hartree−Fock (HF) or DFT calculations with the 6-31G(d) basis set. While the predicted structures of SiNTs are, as expected, sensitive to the theory and/or parameters used, we found a particular mode of structural distortion, which may be termed "gearlike," common to all three types (zigzag, armchair, and chiral) of silicon nanotubes.

2. Model Design and Computational Details

2.1. Design of the Models. To reveal the structural and energetic features of different types of SiNTs, we selected various representative models with different diameters and helicities. The hypothetical SiNT models were first constructed by folding a 2D graphene-like sheet of silicon with a Si−Si bond distance of 2.35 Å. In labeling these SiNTs we adopted the convention commonly used for CNTs.[2]

Specifically, the model SiNTs studied in this work included the zigzag $(n,0)$ structures with $n \in (2,16)$, the armchair (n,n) structures with $n \in (2,8)$, and the chiral (n,m) structures with $n \in (2,4)$ and $m \in (3,6)$. The calculations were performed using both the *periodic* boundary condition (supercell) and the finite *cluster* approach. For the latter, hydrogen atoms were used to terminate the open ends of the SiNTs so as to saturate the dangling bonds, and thus avoiding unwanted distortions, at the ends.

2.2. Theory and Computational Details. Molecular dynamics (MD) simulations of large systems such as those considered here are rather difficult to perform with any first-principle approaches due to the large numbers of atoms involved. Hence, we employed an alternative nonorthogonal density functional tight-binding molecular dynamics simulation scheme,[24−25] hereafter referred to as DFTB-MD, in this work. The DFTB-MD scheme has been found to be highly transferable for a wide variety of systems composed of elements in the first three periods of the Periodic Table. This method utilizes a density functional approach in the calculation of interatomic interactions. It provides an optimal compromise of accuracy, system size, and computation time in comparison to ab initio methods or MD methods using empirical potentials. In addition, Γ point Brillouin zone sampling was used in the total-energy calculations. The suitability of the DFTB approach was verified by calculating the band gap and the Si−Si bond distance of a model silicon crystal containing 64 Si atoms in a supercell. The calculated values of 1.26 eV and 2.36 Å, respectively, were found to be in good agreement with the experimental values of 1.12 eV and 2.35 Å. In the MD simulations, the time step was chosen to be 1 fs, which is adequate and widely used in simulations of atomic motions. The SiNTs described above were equilibrated at various temperatures ranging from 0 to 100 K for 0.5 ps, followed by conjugated gradient relaxation. The atomic force tolerance was limited to 5×10^{-4} eV/Å. The supercell parameter in the tubular axial dimension was optimized to reach an energy tolerance of 0.001 eV/atom. The SiNTs were placed in supercells with spacings (in the *xy* plane, perpendicular to the tube axis along the *z* direction) of at least 10 Å between them. These spacings were found to be large enough to prevent interactions between SiNTs in the lateral (*xy*) plane (i.e., other SiNTs placed in neighboring super cells).

In addition, calculations at HF/6-31G(d) and B3LYP/6-31G-(d) levels of theory were carried out using the Gaussian 98 package[26] for a few select SiNTs, and the results were compared with those obtained via DFTB-MD simulations.
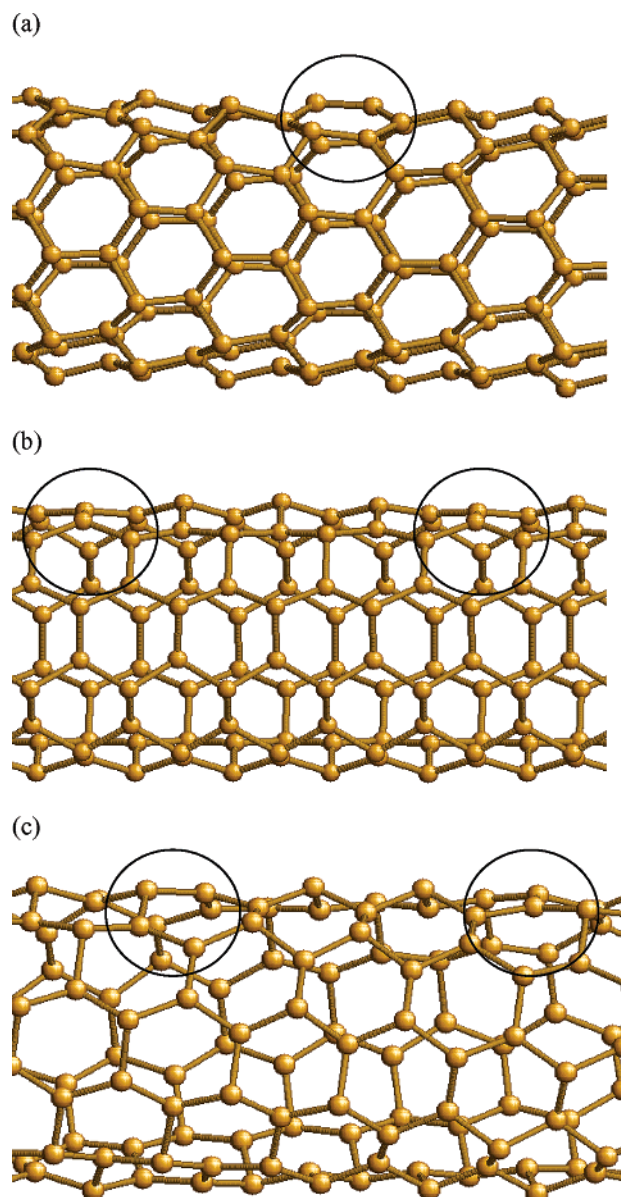
(a)

(b)

(c)

Figure 1. Structures of (a) zigzag (9,0), (b) armchair (5,5), and (c) chiral (4,6) SiNTs annealed from 30 to 0 K for 0.5 ps.

3. Results and Discussion

3.1. Structures of SiNTs. Molecular dynamic simulations were performed on the following representative SiNTs: the zigzag nanotubes $(n,0)$ with $n \in (2,16)$, the armchair nanotubes (n,n) with $n \in (2,8)$, and the chiral nanotubes (n,m) with $n \in (2,4)$ and $m \in (3,6)$.

At 0 K, it was found that SiNTs deviate only slightly from the smooth-walled structures analogous to those of CNTs. However, when the temperature was raised to 10−30 K, considerable structural deformation can occur. Further annealing at higher temperatures eventually led to the collapse of many of the SiNTs. In particular, it was observed that, while small-diameter zigzag SiNTs (for $n < 6$) easily collapse in the temperature range of 10−30 K, SiNTs with larger diameters can usually withstand higher temperatures in the annealing process.

The resulting structures (after annealing and energy optimization as described above) for three representative SiNTs, namely, the zigzag (9,0), the armchair (5,5), and the chiral (4,6) SiNTs, are portrayed in Figure 1a−c, respectively. As we shall also
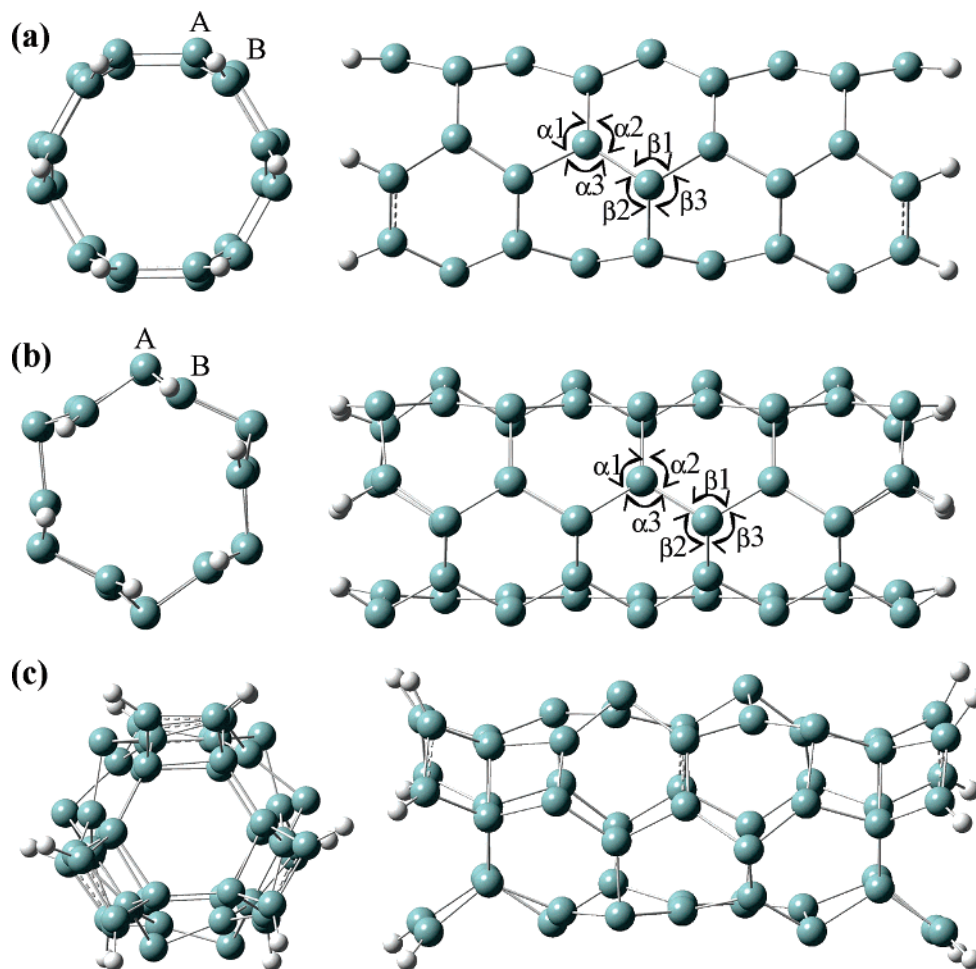
Investigation of Possible Structures of SiNTs

J. Phys. Chem. B, Vol. 109, No. 18, 2005 **8607**

Figure 2. Optimization of the structure of the armchair (3,3) SiNT with ab initio calculations at the HF/6-31G(d) level starting with the structures of (a) a smooth tube analogous to CNT, (b) the gearlike configuration obtained by performing MD, and (c) string-bean-like puckering obtained by using PM3.

see in Figures 2 and 3 (vide infra), the most interesting structural characteristic of these SiNTs is the "gearlike" distortion. The term gearlike distortion refers to the deformation of the tubular structure in such a way that a cross-sectional view (viewed along the tube axis) resembles that of a gear. This kind of distortion will be hereafter described as gearlike, and the resulting configuration as gearlike structure. It was found that all three types of SiNTs exhibit similar gearlike distortion patterns. We note that an analogous structural feature had been noted by Seifert et. al.,[7] using the DFTB method, for negatively charged silicides.

Some deviation from the idealized gearlike configuration, however, can occur, as indicated by the circles in Figure 1. These deviations represent local "defects" of the structures, as a result of the molecular dynamics simulation of the annealing process.

To explore the sensitivity of the results with respect to the calculation method used, we performed geometrical optimizations at three different levels of theoretical sophistication, namely, HF/6-31G(d), B3LYP/6-31G(d), and DFTB, on the armchair (3,3) SiNTs, starting with the structures of (a) a smooth tube analogous to CNT (as used in ref 10), (b) a gearlike configuration obtained by performing MD, and (c) a string-bean-like configuration obtained by using PM3.[19] The numerical results for case a, the structure optimized directly from a smooth tube analogous to CNT (called "direct" in Table 1), and case b, the gearlike structure optimized starting from the gearlike structure obtained via DFTB-MD (called "after MD" in Table 1), after geometrical optimizations via HF/6-31G(d), B3LYP/

6-31G(d), and DFTB, are summarized in Table 1. The results for the string-bean-like configuration (case c) were omitted because the structure was highly distorted. Parts a−c of Figure 2 depict the resulting structures from the three starting models obtained after geometrical optimizations via HF/6-31G(d). The structures from the other two methods (B3LYP/6-31G(d) and DFTB) are similar and will not be shown here.

Results of our calculations show that there are basically two kinds of local configurations for the silicon atoms in the first two kinds of SiNTs (see Figure 2a,b): one being close to tetrahedral (site "A") and the other more-or-less planar (site "B"), regardless of whether the structure is obtained from direct optimization or by application of MD before optimization (see Table 1). It can also be seen from Table 1 that the B3LYP and DFTB methods produce structural parameters very similar to those obtained from the HF theory. Also listed in Table 1 are the sums of angles surrounding type "A" atoms ($\Sigma\alpha = \alpha1 + \alpha2 + \alpha3$) and those surrounding type "B" atoms ($\Sigma\beta = \beta1 + \beta2 + \beta3$), as well as the energies obtained from HF, B3LYP, and DFTB calculations (see Figure 2a,b for definitions of the angles). It can be seen that the sums of angles $\Sigma\alpha$ obtained from geometrical optimization only are larger than the ideal value of 328.4° for a tetrahedral structure (sp^3-like hybridization), whereas the angles from MD plus geometrical optimization are in general significantly smaller. In contrast, the sums of angles $\Sigma\beta$ obtained from both methods are all very close to the idealized value of 360° for a planar structure (sp^2-like hybridization).
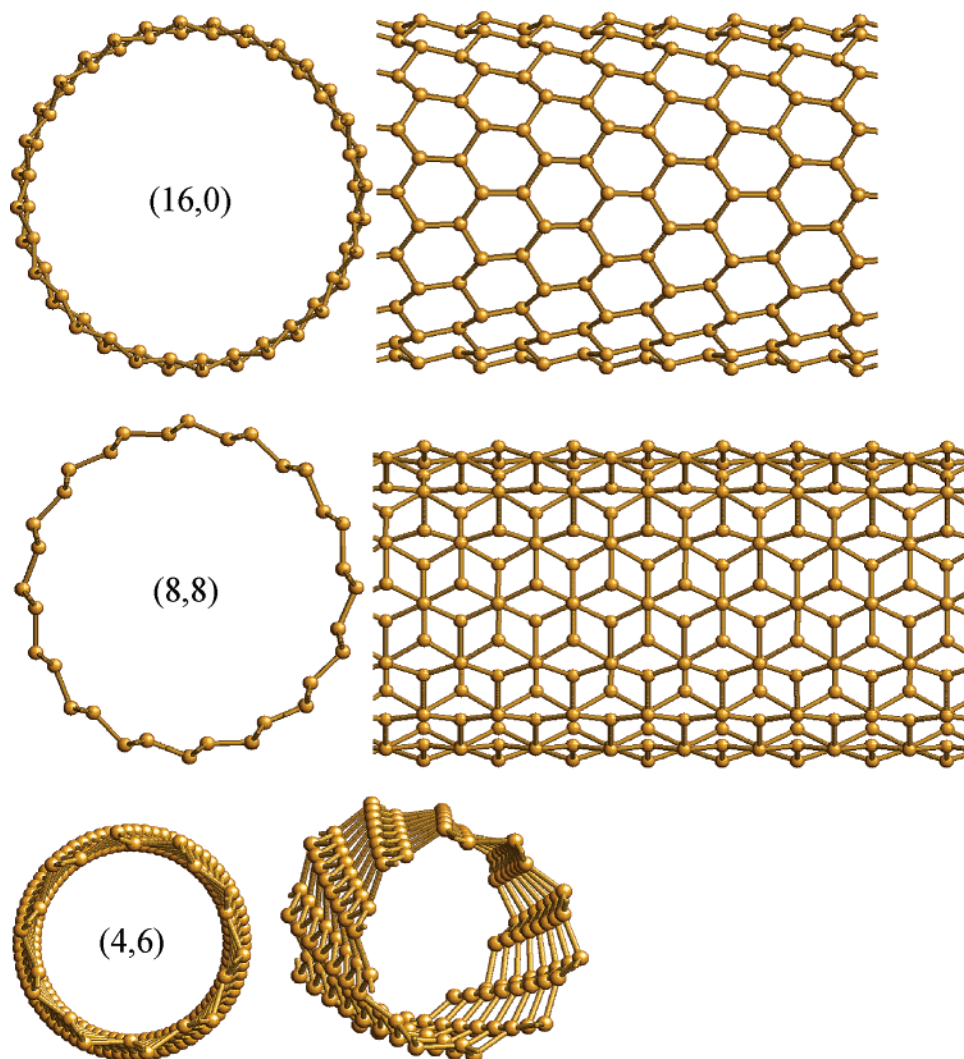
Figure 3. Optimized structures of (a) zigzag (16,0); (b) armchair (8,8), and (c) chiral (4,6) SiNTs.

TABLE 1: Sums of Bond Angles around Type "A" (Σα) and Type "B" (Σβ) Silicon Atoms and Total Energies Obtained from HF, B3LYP, and DFTB Calculations for the Smooth-Tube and the Gearlike (3,3) SiNTs (Corresponding to Figure 2a,b, Respectively)[a]

theory	optimization	Σα (deg)	Σβ (deg)	energy (au)
HF/6-31G(d)	direct[b]	341.3	355.0	-15 607.644 05
	after MD[c]	311.9	359.0	-15 607.892 41
B3LYP/6-31G(d)	direct[b]	335.9	356.8	-15 639.550 79
	after MD[c]	314.4	358.1	-15 639.723 18
DFTB	direct[b]	334.3	356.4	-120.652 392 18
	after MD[c]	305.3	355.1	-121.341 967 95 au
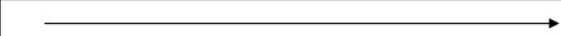
[a] Note that, in our DFTB calculations, a supercell containing 96 Si atoms was used for (3,3) SiNTs and only valence electrons were considered. [b] The geometric optimization was conducted directly from a smooth tube analogous to CNT. [c] The geometric optimization was conducted starting from the gearlike structure that was obtained via DFTB-MD.

Our results also show that the gearlike configuration (Figure 2b) is energetically more favorable than the one obtained by direct optimization of the smooth tube CNT-like structure (Figure 2a) using HF (by 6.75 eV) or DFT (by 4.69 eV). The DFTB method also gives the same trend. It is possible that SiNTs possess a number of energy minima and that a direct optimization only identifies one of the local minima. MD simulation, however, enables the structure, under appropriate conditions, to overcome the energetic barriers in search of other minima, and ultimately, the global energy minimum. Interest-

ingly, the string-bean-like structure (Figure 2c), derived previously by us using the approximate PM3 method[19] (though with some further puckering in the HF and B3LYP calculations reported here), is energetically even more favorable than the two previously mentioned structures (Figure 2a,b). Hence, the string-bean-like structure should be taken as a viable structural type for single-walled SiNTs. However, this particular energetic comparison is somewhat problematic since there are four-membered rings formed at the ends of the tube using the finite cluster model. In other words, the "end effects" of the finite cluster model may have facilitated the string-bean-like structural deformation. Here the end effects of the cluster model refer to the capping of the open ends of the SiNTs with hydrogens and the inevitable structural distortions caused (such as formation of the four-membered rings). These "end effects" may also propagate through the tube axis and cause modulated structural deformation, resulting in the corrugated "string-bean-like" structure with modulated tube diameter.

In principle, one could design SiNTs with similar string-bean-like structures but with longer tube lengths or use the infinite tube model with periodic boundary condition to get around this problem and hope that the structures so-built would be stable under mild annealing conditions with MD. However, such structural features were not observed (i.e., unstable) in our molecular dynamic simulations with infinite periodic models. One reason may be that mild annealing does not provide enough

Investigation of Possible Structures of SiNTs

J. Phys. Chem. B, Vol. 109, No. 18, 2005 **8609**

TABLE 2: Degree of Distortion of Silicon Nanotubes as a Function of the Idealized Hybridizations of the Si−Si Bond, Producing Various Possible Structures

Structure types	Smooth CNT-like tube	Gear-like puckering	String-bean-like distortion	Severe distortion	Collapsed tube
Degree of distortion	$\longrightarrow$				
Structural feature[a]	(image)	(image)	(image)	(image)	(image)
Si-Si bond hybridization[b]	sp^2-sp^2	sp^2-sp^3	sp^2-sp^3	sp^3-sp^3	sp^3-sp^3

[a] Viewed along the tube axis (with the exception of the string-bean-like distortion where the view is perpendicular to the tube axis). [b] Approximate hybridization schemes for two different types (A and B) of Si atoms. See text for details.

deformation to form a stable string-bean-like structure (a local minimum), whereas strong annealing conditions tend to lead to severe distortion and/or collapse of the tube.

In short, the structures of SiNTs are sensitive to the initial models adopted, in addition to their being strongly dependent upon the theory used. This is especially true if one uses geometric optimization only. Our theoretical results, as well as those of others, can be taken as indications that the structures of SiNTs could be wide-ranging and have a number of local minima.

Table 2 shows schematically the structural features and the extents of distortion of the various possible structures of SiNTs. The CNT-like structure is that of a smooth tubular shape and represents a local energy minimum for a given type of silicon nanotube. It is of high structural symmetry and contains predominantly sp^2−sp^2 Si−Si bonding. The gearlike structure is that of a deformed tubular shape and represents an energetically more favorable local minimum. The wavelike deformation occurs at the perimeter (circumference) of the circular cross-section of the tube (perpendicular to the tube axis), giving rise to the gearlike shape of the cross-section. It is of good structural order and reasonably high symmetry and contains mostly sp^2−sp^3 Si−Si bonding. The string-bean-like structure involves even more distortion. The puckering is along the tube axis, giving rise to the corrugated surface with periodically varying tube diameter. Energetically it is more favorable. It also contains mostly sp^2−sp^3 Si−Si bonding. Progressively more severe distortion results in the disruption of the tubular structure, though it may be energetically more favorable because of the increased number of sp^3−sp^3 Si−Si bonding. And finally, total collapse of the tube might occur when the distortion becomes so severe that the structure no longer looks like a tube but rather resembles that of amorphous sp^3 silicon. The final stages of the tube collapse are often associated with an increase in the coordination numbers (i.e., from three, sp^2-like, or four, sp^3-like, to four or higher), resulting in a kind of "implosion".[27] Interestingly, as pointed out by Fagan et al.,[27] CNTs, in their thermal disintegration process, prefer predominantly coordination numbers of three (sp^2) or less, thereby resulting in a kind of "explosion" instead.

3.2. "Gearlike" SiNTs. The gearlike configuration seems to be the dominant structure in our simulations. However, due to local fluctuations in the MD simulation, it is sometimes difficult to obtain structures that are perfectly gearlike. We scanned the simulation temperatures for select SiNTs from 0 to 500 K and found that there is always some degree of disorder (structural defects) in the gearlike structures as evident in Figure 1
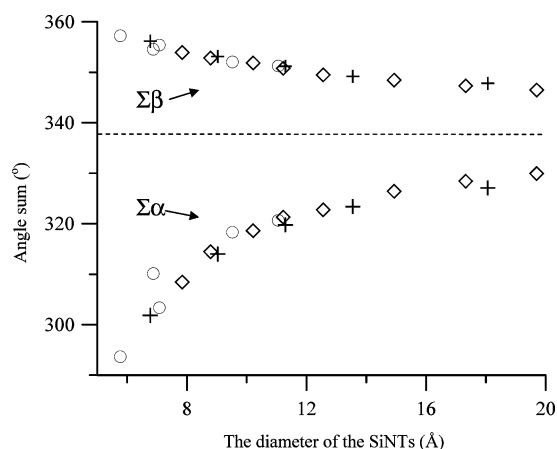
Figure 4. Sums of bond angles $\Sigma\alpha$ (=$\alpha1 + \alpha2 + \alpha3$) and $\Sigma\beta$ (=$\beta1 + \beta2 + \beta3$) vs the diameter of the SiNTs. The data points are "◇" for zigzag $(n,0)$, "+" for armchair (n,n), and "○" for chiral (n,m) SiNTs.

(indicated by circles). In some cases, to minimize the disorder and/or to avoid the collapse of the tube, we had to resort to manually design the initial models in the gearlike configuration. The model structures were then subjected to structural relaxation using DFTB. The final structures of three representative SiNTs, namely, the zigzag (16,0), the armchair (8,8), and the chiral (4,6) SiNTs, are portrayed in Figure 3a−c, respectively. The gearlike configurations of the cross-sections of these SiNTs can readily be seen in the figures.

As stated earlier, our results show that the annealed and optimized SiNTs contain two alternating silicon sites "A" and "B". Site A is close to tetrahedral, while site B is approximately trigonal planar, as indicated by the sums of bond angles, $\Sigma\alpha$ and $\Sigma\beta$. Here, $\Sigma\alpha$ and $\Sigma\beta$ designate the sums of the three angles around site A and site B silicon atoms (see Figure 2), respectively. Figure 4 shows the variation of $\Sigma\alpha$ and $\Sigma\beta$ as functions of the tube diameter. A sum close to the ideal value of $3 \times 109.47° = 328.4°$ is taken here as an indication of a tetrahedral structure (with sp^3-like hybridization), whereas a sum close to the ideal value of $3 \times 120° = 360°$ is indicative of a trigonal-planar structure (with sp^2-like hybridization). It can be seen from Figure 4 that $\Sigma\alpha$ and $\Sigma\beta$ are generally independent of the type or chirality of the SiNTs. They are, however, highly dependent on the diameter of the tube. When the tube diameter exceeds 15 Å, $\Sigma\alpha$ and $\Sigma\beta$ values level off asymptotically to 335 and 340°, respectively, indicating that the angle sums of the two sites (A and B) approach one another as the diameter
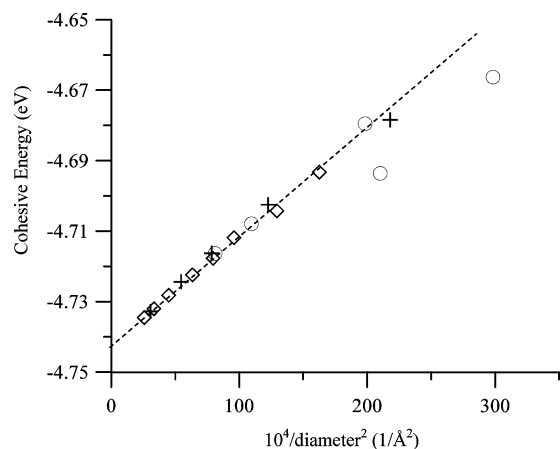
8610 *J. Phys. Chem. B, Vol. 109, No. 18, 2005*

Zhang et al.

Figure 5. Cohesive energy vs 10^4/diameter^2 for the SiNTs. The data points are "◇" for zigzag $(n,0)$, "+" for armchair (n,n), and "○" for chiral (n,m) SiNTs.

increases. As a result, the tube becomes smoother. However, the seemingly noncrossing nature of the two curves, $\Sigma\alpha$ and $\Sigma\beta$, implies that, barring an abrupt structural change, the two sites (A and B) will never coalesce, even with a very large diameter.

To test the "stability" of the calculated SiNTs at higher temperatures, we also performed MD on select optimized gearlike SiNTs at 500 K for 0.5 ps. It was found that many of the SiNTs maintain the gearlike configuration, especially those with large diameters. It should be mentioned that the thermal stabilities of smooth SiNTs (constructed based on CNT-like structures) at various temperatures had been studied by Fagan et al.[27] using Monte Carlo simulations with the empirical Tersoff's potential. It was found by these authors that the (10,0) SiNT is stable up to 1700 K but begins to collapse at temperatures higher than 2200 K. (For comparison, the "disintegration" temperature range for the corresponding CNT was calculated to be around 5500−6000 K [27]).

Figure 5 shows the variation of cohesive energies of the relaxed gearlike SiNTs as a function of the diameter of the tube. It can be seen that the cohesive energy varies linearly with the inverse of the square of the tube diameter, regardless of the type (zigzag, armchair, or chiral) of the SiNT. The cohesive energy approaches asymptotically a value of about 4.74 eV (the intercept in Figure 5) per silicon atom as the diameter increases. We attribute the insensitivity of the cohesive energy with regard to the structure type (zigzag, armchair, or chiral) to the similar local structures for each of the two respective types (A and B) of silicon atoms (see Figure 4) in the relaxed SiNTs with approximately the same diameter.

It should be cautioned, however, that the cohesive energy in Figure 5 refers to the cohesive energy of the nanotube and may be somewhat different from those defined by others. For example, Barnard and Russo[9] defined "strain energy" and "cohesive energy" (both as per atom) of a nanotube as follows:

$$E_{tube} = E_{strain} + E_{cohesive} \tag{1}$$

where E_{tube} is the energy per atom in the tube, as calculated explicitly with DFT. (See also the work of Gao et al.[28]) Here, the strain energy is the "bend energy" per atom required to curve a planar hexagonal sheet, and the cohesive energy is the "stretch energy" per atom in a flat, infinite, two-dimensional (2D) hexagonal sheet. Furthermore, it was shown by these authors that the strain energy and cohesive energy (eq 1) can be obtained

from the slope and intercept of a linear fit to the energy per atom, E_{tube}, versus $1/R^2$, respectively.[9]

It is thus obvious that our definition of cohesive energy (as plotted in Figure 5) refers to E_{tube} in eq 1, whereas that of Barnard and Russo[9] refers to $E_{cohesive}$. To avoid confusion, we shall hereafter denote $E_{cohesive}$ in eq 1 as $E_{2Dcohesive}$. Nevertheless, by adopting the procedure of Barnard and Russo,[9] we can calculate, in our case, the strain (or bend) energy, E_{strain}, required to curve an undulated, ridged, wavelike hexagonal sheet to form the gearlike structure and the corresponding two-dimensional cohesive energy, $E_{2Dcohesive}$, of the undulated, wavelike hexagonal sheet, both from Figure 5. The strain energy of our gearlike SiNTs can be obtained from the slope of the linear fit in Figure 5, which was determined to be 3.07 eV (ignoring the two small-diameter chiral structures). The strain energy is then calculated to be about 0.77 eV. This value is much smaller than the values of 1.782 and 1.494 eV reported by Barnard and Russo[9] for their armchair and the zigzag smooth SiNTs structures (both were based on CNT-like models), respectively. The difference may be attributed to the fact that our strain energy is the bend energy required to curve a ridged or undulated, wavelike hexagonal sheet to form the gearlike structure instead of the bend energy required to roll up a planar hexagonal sheet as in the case of Barnard and Russo.[9]

By the same token, the intercept of the linear fit to Figure 5 gave a value of −4.742 eV for the two-dimensional cohesive (stretch) energy, $E_{2Dcohesive}$, for our ridged or undulated, wavelike hexagonal sheet of silicon. The corresponding $E_{2Dcohesive}$ value for a flat hexagonal silicon sheet, as obtained by Barnard and Russo,[9] is −3.957 eV. The fact that our value is significantly more negative may be a consequence of the undulated structure and a reflection of the tendency of silicon to adopt alternating sp^2- and sp^3-like hybridizations.

In short, the energetic differences between rolling up a ridged or undulated, infinite, two-dimensional hexagonal sheet of silicon to form gearlike SiNTs (this work) and curving a flat sheet to form smooth SiNTs (work of Barnard and Russo[9]) are as follows. First, as can be seen from Figure 5, with the exception of the two small-diameter chiral structures, all three structural types (armchair (n,n), zigzag $(n,0)$, and chiral (n,m)) of single-walled SiNTs fall on the same line, suggesting that the cohesive energy of the tube, E_{tube}, depends only on the tube diameter. This is in sharp contrast to the results of Barnard and Russo[9] which showed that smooth zigzag and armchair SiNTs have different E_{tube} values. Second, as a result of this insensitivity, the strain energies, E_{strain}, are also the same for the three types of structures. This may be taken as an indication that the "energy costs" of curving (rolling up) our ridged or undulated hexagonal sheets of silicon to form the gearlike structures of SiNTs are the same for all three types of structures. This again differs from the results of Barnard and Russo[9] as indicated above. Furthermore, our calculated strain (bend) energy is smaller than those obtained by Barnard and Russo,[9] indicating that the energy cost of rolling up ridged or undulated sheets of silicon to form gearlike structures of SiNTs is significantly less than that for curving a flat sheet to form smooth SiNTs.[9] Finally, the ridged or undulated hexagonal sheet of silicon possesses a larger (absolute) value of $E_{2Dcohesive}$ than that for a flat hexagonal silicon sheet.[9]

Our calculations suggest that all three types of single-walled SiNTs are semiconductors with rather small band gaps (<1 eV), leveling off to fractions of an eV at large diameters, as shown in Figure 6. Contrary to the cohesive energy, the calculated energy gaps seem to depend on the type or chirality of the tube.
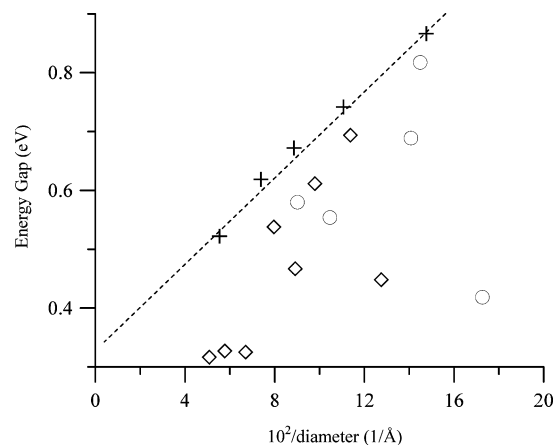
Investigation of Possible Structures of SiNTs

J. Phys. Chem. B, Vol. 109, No. 18, 2005 **8611**

Figure 6. Energy gap vs the 10^2/diameter for the SiNTs. The data points are "◇" for zigzag (n,0), "+" for armchair (n,n), and "○" for chiral (n,m) SiNTs.

However, only the armchair (n,n) SiNTs show a discernible trend. As can be seen from Figure 6, the energy gap of an armchair (n,n) SiNT is linearly proportional to the inverse of the diameter of the tube. It is conceivable that small structural fluctuations in SiNTs may result in seemingly random (small) variation in energy gap. We should also note that the our calculated energy gaps here are considerably smaller than those obtained by Seifert et al. using the DFTB method for silicide and hydrogenated SiNTs.[7]

It is interesting to compare the energy gaps of SiNTs with those of CNTs. As is well-known, SWCNTs may be either metallic or semiconducting. All armchair SWCNTs are metals; those with $n - m = 3k$, where k is a nonzero integer, are semiconductors with a small band gap; and all others are semiconductors with a band gap which is inversely proportional to the nanotube diameter.[2,29,30] Thus, unlike their carbon counterparts (which are metals), armchair (n,n) SiNTs are semiconductors whose band gaps are inversely proportional to the tube diameters. The energy gaps of the zigzag and chiral structures show no discernible trends. However, with the limited set of zigzag SiNTs considered here, the $n - m = 3k$ anomaly also seems to occur, e.g., the band gaps of zigzag (n,0) SiNTs where $n = 3k$ are abnormally small. In sharp contrast to our results, Fagan et al.,[27] through DFT calculations, showed that SiNTs may exhibit metallic (armchair) or semiconductor (zigzag and chiral) behaviors, similar to the corresponding CNTs.

Based on our molecular dynamics simulations, the gearlike SiNTs seem to be the dominant structural form of relaxed SiNTs. However, experimentally, SiNTs are yet to be synthesized. There are two recent experimental observations that are worth mentioning. The first is the preparation of crystalline SiNTs (designated as cSiNTs), which may be described as a hollow crystalline SiNW.[31,32] While this morphology represents a new silicon nanotubular structure, it is very different from the conventional rolled-up graphene-like sheet structures epitomized by the CNTs. In cSiNTs, the silicon atoms are sp^3 hybridized, whereas, in CNTs, the carbon atoms are sp^2 hybridized. The second is the synthesis of a new type of SiC nanostructure,[33] which may be described as SiC nanotube (SiCNT). It was prepared by thermal evaporation (disproportionation) of SiO onto multiwalled CNTs (as a sacrificial template). Element mappings under TEM show a multiwalled tubular structure composed of silicon and carbon atoms. The morphologies of these multiwalled SiCNTs are similar to the conventional rolled-up graphene-like structures of multiwalled CNTs (but with larger interlayer spacings). In other words, the atoms in SiCNTs are

sp^2 hybridized as in CNTs. Finally, it is known that layered silicon systems exist in some silicides. For instance, in alkaline earth metal silicides,[34] the silicon layers, formed by cyclohexane-like rings, are separated by metal ions. It is conceivable that the layered structure of silicon in these systems may roll up to form tubular structures analogous to the gearlike configurations described in this paper.

4. Conclusions

Single-walled silicon nanotubes (SiNTs) may adopt tubular structures with a number of possible local configurations. Our density functional tight-binding molecular dynamics simulations as well as Hartree−Fock and DFT calculations, presented in this paper, suggest that they may adopt gearlike structures containing alternating tetrahedral (with sp^3-like hybridization) and trigonal-planar (with sp^2-like hybridization) local Si configurations. These structures were annealed at moderate temperatures (below 100 K). The resulting gearlike structures of SiNTs deviate considerably from, and are of lower energies than, the smooth-walled SiNTs similar to the single-walled CNTs. They are, however, energetically less favorable than the string-bean-like SiNT structures, which represent yet another set of local energy minima. The energetics and the structures of gearlike SiNTs are shown to depend primarily on the diameter of the tube, irrespective of the type (zigzag, armchair, or chiral). In contrast, the energy gap is very sensitive to both the diameter and the type of the nanotube. All three types (zigzag, armchair, or chiral) of SiNTs were found to be semiconductors with small band gaps ($<$1 eV).

References and Notes

(1) Iijima, S. *Nature (London)* **1991**, *354*, 56.
(2) Saito, R.; Dresselhaus, G.; Dresselhaus, M. S. *Physical Properties of Carbon Nanotubes*; Imperial College Press: London, 1998.
(3) Rubio, A.; Corkill, J. L.; Cohen, M. L. *Phys. Rev. B* **1994**, *49*, R5081.
(4) Miyamoto, Y.; Rubio, A.; Cohen, M. L.; Louie, S. G. *Phys. Rev. B* **1994**, *50*, R4976.
(5) Cote, M.; Cohen, M. L.; Chadi, D. J. *Phys. Rev. B* **1998**, *58*, R4277.
(6) Zhang, D. J.; Zhang, R. Q. *Chem. Phys. Lett.* **2003**, *371*, 426.
(7) Seifert, G.; Kohler, Th.; Urbassek, H. M.; Hernandez, E.; Frauenheim, Th. *Phys. Rev. B* **2001**, *63*, 193409.
(8) Fagan, S. B.; Barierle, R. J.; Mota, R.; da Silva, A. J. R.; Fazzio, A. *Phys. Rev. B* **2000**, *61*, 9994.
(9) Barnard, A. S.; Russo, S. P. *J. Phys. Chem. B* **2003**, *107*, 7577.
(10) Zhang, M.; Kan, Y. H.; Zang, Q. J.; Su, Z. M.; Wang, R. S. *Chem. Phys. Lett.* **2003**, *379*, 81.
(11) Kang, J. W.; Hwang, H. J. *Nanotechnology* **2003**, *14*, 402.
(12) Kang, J. W.; Byun, K. R.; Hwang, H. J. *Modelling Simul. Mater. Sci. Eng.* **2004**, *12*, 1.
(13) Bai, J.; Zeng, X. C.; Tanaka, H.; Zeng, J. Y. *Proc. Natl. Acad. Sci. U.S.A.* **2004**, *101*, 2664.
(14) Wang, N.; Tang, Y. H.; Zhang, Y. F.; Lee, C. S.; Lee, S. T. *Phys. Rev. B* **1998**, *58*, R16024.
(15) Hu, J.; Ouyang, M.; Yang, P.; Lieber, C. M. *Nature (London)* **1999**, *399*, 48.
(16) Menon, M.; Richter, E. *Phys. Rev. Lett.* **1999**, *83*, 792.
(17) Marsen, B.; Sattler, K. *Phys. Rev. B* **1999**, *60*, 11593.
(18) Landman, U.; Barnett, R. N.; Scherbakov, A. G.; Avouris, P. *Phys. Rev. B* **2000**, *61*, 9994.
(19) Zhang, R. Q.; Lee, S. T.; Law, C. K.; Li, W. K.; Teo, B. K. *Chem. Phys. Lett.* **2002**, *364*, 251.
(20) Leobandung, E.; Guo, L.; Chou, S. Y. *Appl. Phys. Lett.* **1997**, *67*, 938.

(21) Zhang, X. Y.; Zhang, L. D.; Meng, G. W.; Li, G. H.; Yun, N.; Phillipp, J.; Phillipp, E. *Adv. Mater.* **2001**, *13*, 1238.

(22) Lee, S. T.; Zhang, R. Q.; Lifshitz, Y. In *Nanowires and Nanobelts: Materials, Properties and Devices*; Wang, Z. L., Ed.; Kluwer Academic/Plenum: New York, 2003; pp 397−446, and references therein.

(23) Zhang, R. Q.; Lifshitz, Y.; Lee, S. T. *Adv. Mater.* **2003**, *15*, 639, and references therein.

(24) Elstner, M.; Porezag, D.; Jungnickel, G.; Elsner, J.; Haugk, M.; Frauenheim, Th.; Suhai, S.; Seifert, G. *Phys. Rev. B* **1998**, *58*, 7260.

(25) Frauenheim, Th.; Seifert, G.; Elstner, M.; Hajnal, Z.; Jungnickel, G.; Porezag, D.; Suhai, S.; Scholz, R. *Phys. Status Solidi B* **2000**, *217*, 41.

(26) Frisch, M. J.; Trucks, G. W.; Schlegel, H. B.; Scuseria, G. E.; Robb, M. A.; Cheeseman, J. R.; Zakrzewski, V. G.; Montgomery, J. A., Jr.; Stratmann, R. E.; Burant, J. C.; Dapprich, S.; Millam, J. M.; Daniels, A. D.; Kudin, K. N.; Strain, M. C.; Farkas, O.; Tomasi, J.; Barone, V.; Cossi, M.; Cammi, R.; Mennucci, B.; Pomelli, C.; Adamo, C.; Clifford, S.; Ochterski, J.; Petersson, G. A.; Ayala, P. Y.; Cui, Q.; Morokuma, K.; Malick, D. K.; Rabuck, A. D.; Raghavachari, K.; Foresman, J. B.; Cioslowski, J.; Ortiz, J. V.; Baboul, A. G.; Stefanov, B. B.; Liu, G.; Liashenko, A.; Piskorz, P.; Komaromi, I.; Gomperts, R.; Martin, R. L.; Fox, D. J.; Keith, T.; Al-Laham, M. A.; Peng, C. Y.; Nanayakkara, A.; Gonzalez, C.; Challacombe, M.; Gill, P. M. W.; Johnson, B.; Chen, W.; Wong, M. W.; Andres, J. L.; Gonzalez, C.; Head-Gordon, M.; Replogle, E. S.; Pople, J. A. *Gaussian 98*, Revision A.11; Gaussian, Inc.: Pittsburgh, PA, 2001.

(27) Fagan, S. B.; Mota, R.; Baierle, R. J.; Paiva, G.; da Silva, A. J. R.; Fazzio, A. *J. Mol. Struct. (THEOCHEM)* **2001**, *539*, 101.

(28) Gao, G.; Cagin, T.; Goddard, W. A., III *Nanotechnology* **1998**, *9*, 184.

(29) Harigaya, K. *Phys. Rev. B* **1992**, *45*, 12071.

(30) Louie, S. G. *Top. Appl. Phys.* **2001**, *80*, 113.

(31) Sha, J.; Niu, J. J.; Ma, X. Y. *Adv. Mater.* **2002**, *14*, 1219.

(32) Teo, B. K.; Li, C. P.; Sun, X. H.; Wong, N. B.; Lee, S. T. *Inorg. Chem.* **2003**, *42*, 6723.

(33) Sun, X. H.; Li, C. P.; Wong, W.-K.; Wong, N.-B.; Lee, C.-S.; Lee, S.-T.; Teo, B.-K. *J. Am. Chem. Soc.* **2002**, *124*, 14464.

(34) Janzon, K. H.; Schafer, H.; Weiss, A. *Z. Anorg. Allg. Chem.* **1970**, *372*, 87.